MIT Libraries | DSpace@MIT

MIT Open Access Articles

Search for Resonances Decaying to Top and Bottom Quarks with the CDF Experiment

The MIT Faculty has made this article openly available. ***Please share*** how this access benefits you. Your story matters.

Citation: Aaltonen, T., et al. "Search for Resonances Decaying to Top and Bottom Quarks with the CDF Experiment." Phys. Rev. Lett. 115, 061801 (August 2015). © 2015 American Physical Society

As Published: http://dx.doi.org/10.1103/PhysRevLett.115.061801

Publisher: American Physical Society

Persistent URL: http://hdl.handle.net/1721.1/98009

Version: Final published version: final published article, as it appeared in a journal, conference proceedings, or other formally published context

Terms of Use: Article is made available in accordance with the publisher's policy and may be subject to US copyright law. Please refer to the publisher's site for terms of use.

Massachusetts Institute of Technology

Search for Resonances Decaying to Top and Bottom Quarks with the CDF Experiment

T. Aaltonen,[21] S. Amerio,[39a,39b] D. Amidei,[31] A. Anastassov,[15,w] A. Annovi,[17] J. Antos,[12] F. Anzà,[38] G. Apollinari,[15] J. A. Appel,[15] T. Arisawa,[52] A. Artikov,[13] J. Asaadi,[47] W. Ashmanskas,[15] B. Auerbach,[2] A. Aurisano,[47] F. Azfar,[38] W. Badgett,[15] T. Bae,[25] A. Barbaro-Galtieri,[26] V. E. Barnes,[43] B. A. Barnett,[23] P. Barria,[41a,41c] P. Bartos,[12] M. Bauce,[39a,39b] F. Bedeschi,[41a] S. Behari,[15] G. Bellettini,[41a,41b] J. Bellinger,[54] D. Benjamin,[14] A. Beretvas,[15] A. Bhatti,[45] L. Bianchi,[15] K. R. Bland,[5] B. Blumenfeld,[23] A. Bocci,[14] A. Bodek,[44] D. Bortoletto,[43] J. Boudreau,[42a] A. Boveia,[11] L. Brigliadori,[6a,6b] C. Bromberg,[32] E. Brucken,[21] J. Budagov,[13] H. S. Budd,[44] K. Burkett,[15] G. Busetto,[39a,39b] P. Bussey,[19] P. Butti,[41a,41b] A. Buzatu,[19] A. Calamba,[10] S. Camarda,[4] M. Campanelli,[28] F. Canelli,[11,dd] B. Carls,[22] D. Carlsmith,[54] R. Carosi,[41a] S. Carrillo,[16,l] B. Casal,[9,j] M. Casarsa,[48a] A. Castro,[6a,6b] P. Catastini,[20] D. Cauz,[48a,48b,48c] V. Cavaliere,[22] A. Cerri,[26,e] L. Cerrito,[28,r] Y. C. Chen,[1] M. Chertok,[7] G. Chiarelli,[41a] G. Chlachidze,[15] K. Cho,[25] D. Chokheli,[13] A. Clark,[18] C. Clarke,[53] M. E. Convery,[15] J. Conway,[7] M. Corbo,[15,z] M. Cordelli,[17] C. A. Cox,[7] D. J. Cox,[7] M. Cremonesi,[41a] D. Cruz,[47] J. Cuevas,[9,y] R. Culbertson,[15] N. d'Ascenzo,[15,v] M. Datta,[15,gg] P. de Barbaro,[44] L. Demortier,[45] M. Deninno,[6a] M. D'Errico,[39a,39b] F. Devoto,[21] A. Di Canto,[41a,41b] B. Di Ruzza,[15,p] J. R. Dittmann,[5] S. Donati,[41a,41b] M. D'Onofrio,[27] M. Dorigo,[48a,48d] A. Driutti,[48a,48b,48c] K. Ebina,[52] R. Edgar,[31] A. Elagin,[47] R. Erbacher,[7] S. Errede,[22] B. Esham,[22] S. Farrington,[38] J. P. Fernández Ramos,[29] R. Field,[16] G. Flanagan,[15,t] R. Forrest,[7] M. Franklin,[20] J. C. Freeman,[15] H. Frisch,[11] Y. Funakoshi,[52] C. Galloni,[41a,41b] A. F. Garfinkel,[43] P. Garosi,[41a,41c] H. Gerberich,[22] E. Gerchtein,[15] S. Giagu,[46a] V. Giakoumopoulou,[3] K. Gibson,[42a] C. M. Ginsburg,[15] N. Giokaris,[3] P. Giromini,[17] V. Glagolev,[13] D. Glenzinski,[15] M. Gold,[34] D. Goldin,[47] A. Golossanov,[15] G. Gomez,[9] G. Gomez-Ceballos,[30] M. Goncharov,[30] O. González López,[29] I. Gorelov,[34] A. T. Goshaw,[14] K. Goulianos,[45] E. Gramellini,[6a] C. Grosso-Pilcher,[11] R. C. Group,[51,15] J. Guimaraes da Costa,[20] S. R. Hahn,[15] J. Y. Han,[44] F. Happacher,[17] K. Hara,[49] M. Hare,[50] R. F. Harr,[53] T. Harrington-Taber,[15,m] K. Hatakeyama,[5] C. Hays,[38] J. Heinrich,[40] M. Herndon,[54] A. Hocker,[15] Z. Hong,[47] W. Hopkins,[15,f] S. Hou,[1] R. E. Hughes,[35] U. Husemann,[55] M. Hussein,[32,bb] J. Huston,[32] G. Introzzi,[41a,41e,41f] M. Iori,[46a,46b] A. Ivanov,[7,o] E. James,[15] D. Jang,[10] B. Jayatilaka,[15] E. J. Jeon,[25] S. Jindariani,[15] M. Jones,[43] K. K. Joo,[25] S. Y. Jun,[10] T. R. Junk,[15] M. Kambeitz,[24] T. Kamon,[25,47] P. E. Karchin,[53] A. Kasmi,[5] Y. Kato,[37,n] W. Ketchum,[11,hh] J. Keung,[40] B. Kilminster,[15,dd] D. H. Kim,[25] H. S. Kim,[25] J. E. Kim,[25] M. J. Kim,[17] S. H. Kim,[49] S. B. Kim,[25] Y. J. Kim,[25] Y. K. Kim,[11] N. Kimura,[52] M. Kirby,[15] K. Knoepfel,[15] K. Kondo,[52,*] D. J. Kong,[25] J. Konigsberg,[16] A. V. Kotwal,[14] M. Kreps,[24] J. Kroll,[40] M. Kruse,[14] T. Kuhr,[24] M. Kurata,[49] A. T. Laasanen,[43] S. Lammel,[15] M. Lancaster,[28] K. Lannon,[35,x] G. Latino,[41a,41c] H. S. Lee,[25] J. S. Lee,[25] S. Leo,[22] S. Leone,[41a] J. D. Lewis,[15] A. Limosani,[14,s] E. Lipeles,[40] A. Lister,[18,a] H. Liu,[51] Q. Liu,[43] T. Liu,[15] S. Lockwitz,[55] A. Loginov,[55] D. Lucchesi,[39a,39b] A. Lucà,[17] J. Lueck,[24] P. Lujan,[26] P. Lukens,[15] G. Lungu,[45] J. Lys,[26] R. Lysak,[12,d] R. Madrak,[15] P. Maestro,[41a,41c] S. Malik,[45] G. Manca,[27,b] A. Manousakis-Katsikakis,[3] L. Marchese,[6a,ii] F. Margaroli,[46a] P. Marino,[41a,41d] K. Matera,[22] M. E. Mattson,[53] A. Mazzacane,[15] P. Mazzanti,[6a] R. McNulty,[27,i] A. Mehta,[27] P. Mehtala,[21] C. Mesropian,[45] T. Miao,[15] D. Mietlicki,[31] A. Mitra,[1] H. Miyake,[49] S. Moed,[15] N. Moggi,[6a] C. S. Moon,[15,z] R. Moore,[,ee15,ff] M. J. Morello,[41a,41d] A. Mukherjee,[15] Th. Muller,[24] P. Murat,[15] M. Mussini,[6a,6b] J. Nachtman,[15,m] Y. Nagai,[49] J. Naganoma,[52] I. Nakano,[36] A. Napier,[50] J. Nett,[47] C. Neu,[51] T. Nigmanov,[42a] L. Nodulman,[2] S. Y. Noh,[25] O. Norniella,[22] L. Oakes,[38] S. H. Oh,[14] Y. D. Oh,[25] I. Oksuzian,[51] T. Okusawa,[37] R. Orava,[21] L. Ortolan,[4] C. Pagliarone,[48a] E. Palencia,[9,e] P. Palni,[34] V. Papadimitriou,[15] W. Parker,[54] G. Pauletta,[48a,48b,48c] M. Paulini,[10] C. Paus,[30] T. J. Phillips,[14] G. Piacentino,[15,q] E. Pianori,[40] J. Pilot,[7] K. Pitts,[22] C. Plager,[8] L. Pondrom,[54] S. Poprocki,[15,f] K. Potamianos,[26] A. Pranko,[26] F. Prokoshin,[13,aa] F. Ptohos,[17,g] G. Punzi,[41a,41b] I. Redondo Fernández,[29] P. Renton,[38] M. Rescigno,[46a] F. Rimondi,[6a,*] L. Ristori,[41a,15] A. Robson,[19] T. Rodriguez,[40] S. Rolli,[50,h] M. Ronzani,[41a,41b] R. Roser,[15] J. L. Rosner,[11] F. Ruffini,[41a,41c] A. Ruiz,[9] J. Russ,[10] V. Rusu,[15] W. K. Sakumoto,[44] Y. Sakurai,[52] L. Santi,[48a,48b,48c] K. Sato,[49] V. Saveliev,[15,v] A. Savoy-Navarro,[15,z] P. Schlabach,[15] E. E. Schmidt,[15] T. Schwarz,[31] L. Scodellaro,[9] F. Scuri,[41a] S. Seidel,[34] Y. Seiya,[37] A. Semenov,[13] F. Sforza,[41a,41b] S. Z. Shalhout,[7] T. Shears,[27] P. F. Shepard,[42a] M. Shimojima,[49,u] M. Shochet,[11] I. Shreyber-Tecker,[33] A. Simonenko,[13] K. Sliwa,[50] J. R. Smith,[7] F. D. Snider,[15] H. Song,[42a] V. Sorin,[4] R. St. Denis,[19,*] M. Stancari,[15] D. Stentz,[15,w] J. Strologas,[34] Y. Sudo,[49] A. Sukhanov,[15] I. Suslov,[13] K. Takemasa,[49] Y. Takeuchi,[49] J. Tang,[11] M. Tecchio,[31] P. K. Teng,[1] J. Thom,[15,f] E. Thomson,[40] V. Thukral,[47] D. Toback,[47] S. Tokar,[12] K. Tollefson,[32] T. Tomura,[49] D. Tonelli,[15,e] S. Torre,[17] D. Torretta,[15] P. Totaro,[39a] M. Trovato,[41a,41d] F. Ukegawa,[49] S. Uozumi,[25] F. Vázquez,[16,l] G. Velev,[15] C. Vellidis,[15] C. Vernieri,[41a,41d] M. Vidal,[43] R. Vilar,[9] J. Vizán,[9,cc] M. Vogel,[34] G. Volpi,[17] P. Wagner,[40] R. Wallny,[15,j] S. M. Wang,[1] D. Waters,[28] W. C. Wester III,[15] D. Whiteson,[40,c] A. B. Wicklund,[2] S. Wilbur,[7] H. H. Williams,[40] J. S. Wilson,[31] P. Wilson,[15] B. L. Winer,[35] P. Wittich,[15,f] S. Wolbers,[15] H. Wolfe,[35] T. Wright,[31] X. Wu,[18] Z. Wu,[5] K. Yamamoto,[37] D. Yamato,[37]

 © 2015 American Physical Society

T. Yang,[15] U. K. Yang,[25] Y. C. Yang,[25] W.-M. Yao,[26] G. P. Yeh,[15] K. Yi,[15,m] J. Yoh,[15] K. Yorita,[52] T. Yoshida,[37,k] G. B. Yu,[14] I. Yu,[25] A. M. Zanetti,[48a] Y. Zeng,[14] C. Zhou,[14] and S. Zucchelli[6a,6b]

(CDF Collaboration)

[1]*Institute of Physics, Academia Sinica, Taipei, Taiwan 11529, Republic of China*
[2]*Argonne National Laboratory, Argonne, Illinois 60439, USA*
[3]*University of Athens, 157 71 Athens, Greece*
[4]*Institut de Fisica d'Altes Energies, ICREA, Universitat Autonoma de Barcelona, E-08193, Bellaterra (Barcelona), Spain*
[5]*Baylor University, Waco, Texas 76798, USA*
[6a]*Istituto Nazionale di Fisica Nucleare Bologna, I-40127 Bologna, Italy*
[6b]*University of Bologna, I-40127 Bologna, Italy*
[7]*University of California, Davis, Davis, California 95616, USA*
[8]*University of California, Los Angeles, Los Angeles, California 90024, USA*
[9]*Instituto de Fisica de Cantabria, CSIC-University of Cantabria, 39005 Santander, Spain*
[10]*Carnegie Mellon University, Pittsburgh, Pennsylvania 15213, USA*
[11]*Enrico Fermi Institute, University of Chicago, Chicago, Illinois 60637, USA*
[12]*Comenius University, 842 48 Bratislava, Slovakia; Institute of Experimental Physics, 040 01 Kosice, Slovakia*
[13]*Joint Institute for Nuclear Research, RU-141980 Dubna, Russia*
[14]*Duke University, Durham, North Carolina 27708, USA*
[15]*Fermi National Accelerator Laboratory, Batavia, Illinois 60510, USA*
[16]*University of Florida, Gainesville, Florida 32611, USA*
[17]*Laboratori Nazionali di Frascati, Istituto Nazionale di Fisica Nucleare, I-00044 Frascati, Italy*
[18]*University of Geneva, CH-1211 Geneva 4, Switzerland*
[19]*Glasgow University, Glasgow G12 8QQ, United Kingdom*
[20]*Harvard University, Cambridge, Massachusetts 02138, USA*
[21]*Division of High Energy Physics, Department of Physics, University of Helsinki, FIN-00014, Helsinki, Finland; Helsinki Institute of Physics, FIN-00014, Helsinki, Finland*
[22]*University of Illinois, Urbana, Illinois 61801, USA*
[23]*The Johns Hopkins University, Baltimore, Maryland 21218, USA*
[24]*Institut für Experimentelle Kernphysik, Karlsruhe Institute of Technology, D-76131 Karlsruhe, Germany*
[25]*Center for High Energy Physics, Kyungpook National University, Daegu 702-701, Korea; Seoul National University, Seoul 151-742, Korea; Sungkyunkwan University, Suwon 440-746, Korea; Korea Institute of Science and Technology Information, Daejeon 305-806, Korea; Chonnam National University, Gwangju 500-757, Korea; Chonbuk National University, Jeonju 561-756, Korea; Ewha Womans University, Seoul, 120-750, Korea*
[26]*Ernest Orlando Lawrence Berkeley National Laboratory, Berkeley, California 94720, USA*
[27]*University of Liverpool, Liverpool L69 7ZE, United Kingdom*
[28]*University College London, London WC1E 6BT, United Kingdom*
[29]*Centro de Investigaciones Energeticas Medioambientales y Tecnologicas, E-28040 Madrid, Spain*
[30]*Massachusetts Institute of Technology, Cambridge, Massachusetts 02139, USA*
[31]*University of Michigan, Ann Arbor, Michigan 48109, USA*
[32]*Michigan State University, East Lansing, Michigan 48824, USA*
[33]*Institution for Theoretical and Experimental Physics, ITEP, Moscow 117259, Russia*
[34]*University of New Mexico, Albuquerque, New Mexico 87131, USA*
[35]*The Ohio State University, Columbus, Ohio 43210, USA*
[36]*Okayama University, Okayama 700-8530, Japan*
[37]*Osaka City University, Osaka 558-8585, Japan*
[38]*University of Oxford, Oxford OX1 3RH, United Kingdom*
[39a]*Istituto Nazionale di Fisica Nucleare, Sezione di Padova, I-35131 Padova, Italy*
[39b]*University of Padova, I-35131 Padova, Italy*
[40]*University of Pennsylvania, Philadelphia, Pennsylvania 19104, USA*
[41a]*Istituto Nazionale di Fisica Nucleare Pisa, I-56127 Pisa, Italy*
[41b]*University of Pisa, I-56127 Pisa, Italy*
[41c]*University of Siena, I-53100 Siena, Italy*
[41d]*Scuola Normale Superiore, I-56127 Pisa, Italy*
[41e]*INFN Pavia, I-27100 Pavia, Italy*
[41f]*University of Pavia, I-27100 Pavia, Italy*
[42]*University of Pittsburgh, Pittsburgh, Pennsylvania 15260, USA*

[43]Purdue University, West Lafayette, Indiana 47907, USA
[44]University of Rochester, Rochester, New York 14627, USA
[45]The Rockefeller University, New York, New York 10065, USA
[46a]Istituto Nazionale di Fisica Nucleare, Sezione di Roma 1, I-00185 Roma, Italy
[46b]Sapienza Università di Roma, I-00185 Roma, Italy
[47]Mitchell Institute for Fundamental Physics and Astronomy, Texas A&M University, College Station, Texas 77843, USA
[48a]Istituto Nazionale di Fisica Nucleare Trieste, I-34127 Trieste, Italy
[48b]Gruppo Collegato di Udine, I-33100 Udine, Italy
[48c]University of Udine, I-33100 Udine, Italy
[48d]University of Trieste, I-34127 Trieste, Italy
[49]University of Tsukuba, Tsukuba, Ibaraki 305, Japan
[50]Tufts University, Medford, Massachusetts 02155, USA
[51]University of Virginia, Charlottesville, Virginia 22906, USA
[52]Waseda University, Tokyo 169, Japan
[53]Wayne State University, Detroit, Michigan 48201, USA
[54]University of Wisconsin, Madison, Wisconsin 53706, USA
[55]Yale University, New Haven, Connecticut 06520, USA
(Received 7 April 2015; published 3 August 2015)

We report on a search for charged massive resonances decaying to top (t) and bottom (b) quarks in the full data set of proton-antiproton collisions at a center-of-mass energy of $\sqrt{s} = 1.96$ TeV collected by the CDF II detector at the Tevatron, corresponding to an integrated luminosity of 9.5 fb^{-1}. No significant excess above the standard model background prediction is observed. We set 95% Bayesian credibility mass-dependent upper limits on the heavy charged-particle production cross section times branching ratio to tb. Using a standard model extension with a $W' \to tb$ and left-right-symmetric couplings as a benchmark model, we constrain the W' mass and couplings in the 300–900 GeV$/c^2$ range. The limits presented here are the most stringent for a charged resonance with mass in the range 300–600 GeV$/c^2$ decaying to top and bottom quarks.

DOI: 10.1103/PhysRevLett.115.061801 PACS numbers: 13.85.Rm, 12.60.Cn, 14.65.Ha, 14.80.Rt

Several modifications of the standard model (SM) of particle physics predict the existence of massive, short-lived states decaying to pairs of SM leptons or quarks. Such a resonance decaying to a top (t) and a bottom (b) quark, tb, appears in models such as left-right-symmetric SM extensions [1], Kaluza-Klein extra dimensions [2,3], technicolor [4,5], or little Higgs scenarios [6] featuring one or more massive charged vector bosons, generically denoted as W' . Searches for W' bosons in the $W' \to tb$ decay channel are complementary to searches in the leptonic decay channel $W' \to \ell\nu$, and probe the most general scenario where the couplings of the W' boson to fermions are free parameters.

Recent searches in the $W' \to tb$ channel have been performed by the CDF [7] and D0 [8] Collaborations in proton-antiproton ($p\bar{p}$) collisions at 1.96 TeV c.m. energy at the Tevatron, and by the ATLAS [9] and CMS [10] Collaborations in proton-proton collisions at 8 TeV c.m. energy at the Large Hadron Collider (LHC). For mass scales approaching and surpassing 1 TeV, the LHC experiments have superior sensitivity over the Tevatron experiments due to the enhancement of the production cross section at the higher center-of-mass energy of the collisions. However, in the mass region well below 1 TeV, the Tevatron experiments have greater sensitivity due to the relative suppression of gluon-initiated backgrounds compared to the quark-initiated signals such as the one under consideration here.

In this Letter, we present a novel search for charged massive resonances decaying to the tb quark pair. The search is performed in events where the top quark decays to a Wb pair and the W boson decays to a charged lepton and a neutrino; the two bottom quarks hadronize and produce two clusters of particles (jets). Since no assumptions on the signal model other than on the natural width are made, this search is sensitive to any narrow resonant state decaying to a tb final state. A simple left-right-symmetric SM extension [11], predicting the existence of W' bosons of unknown mass and universal weak-coupling strength to SM fermions, is used as a benchmark model. The reconstructed width of the signal is dominated by resolution effects; the test signal is therefore applicable for any W'-like particle whose width is small compared to the experimental resolution.

The data were collected at the Tevatron $p\bar{p}$ collider at a center-of-mass energy of 1.96 TeV and were recorded by the CDF II detector [12]. The detector consists of a silicon microstrip vertex detector and a cylindrical drift chamber immersed in a 1.4 T magnetic field for vertex and charged-particle trajectory (track) reconstruction, surrounded by pointing-tower-geometry electromagnetic and hadronic calorimeters for energy measurement, and muon detectors outside the calorimeters [13].

We analyze events accepted by the online event selection (trigger) that requires either the event missing transverse energy $\not\!\!E_T$ to satisfy $\not\!\!E_T > 45$ GeV or, alternatively $\not\!\!E_T > 35$ GeV and the presence of two or more jets, each with transverse energy $E_T > 15$ GeV. The full data set corresponds to an integrated luminosity of 9.5 fb^{-1}. Off-line, we select events with $\not\!\!E_T > 50$ GeV, after correcting measured jet energies for instrumental effects [14]. We further require events to have two or three high-E_T jets, where the two jets j_1, j_2 with the largest transverse energies, $E_T^{j_1}$ and $E_T^{j_2}$, are required to satisfy $E_T^{j_1} > 35$ GeV and $E_T^{j_2} > 25$ GeV; the jet energies are determined from calorimeter deposits and corrected using charged-particle momentum measurements [15]. One leading jet is required to be within the silicon detector acceptance, $|\eta| < 0.8$; the other satisfies $|\eta| < 2.0$. In addition to the large missing transverse energy indicating the presence of a high-p_T neutrino, the presence of a W boson decaying to an $e\nu_e$ or $\mu\nu_\mu$ pair is confirmed by requiring a reconstructed electron or muon. Leptonically decaying τ leptons are collected in the same way. Hadronically decaying τ leptons from the W decay chain are mostly reconstructed as jets in the calorimeter. Three-jet events are thus retained, while events with more than three jets with $E_T^j > 15$ GeV and $|\eta| < 2.4$ are excluded. The majority of the background at this stage is quantum chromodynamics (QCD) production of multijet events, which yields $\not\!\!E_T$ generated through jet-energy mismeasurements. Neutrinos produced in semileptonic b-hadron decays also contribute to the $\not\!\!E_T$ of these events. In both cases, the $\vec{\not\!\!E}_T$ is typically aligned with the projection on the transverse plane of the second or third jet momentum. Events are rejected by requiring the azimuthal separation $\Delta\varphi$ between $\vec{\not\!\!E}_T$ and $\vec{E}_{\mathrm{T}}^{j_2}$ (or $\vec{E}_{\mathrm{T}}^{j_3}$) to be larger than 0.4. The resulting sample, *pretag*, contains 391 229 events; about 940 of these would originate from the decay of a 300 GeV/c^2 W' boson with SM-like couplings.

In order to identify jets originated from the hadronization of a b quark ("b tagged"), we use two different algorithms, each tuned either for making a very pure selection (tight), or for making a somewhat less pure selection that is more efficient (loose). The SECVTX algorithm [16] looks for a vertex displaced from the collisions point produced by the in-flight decay of a b-flavored hadron; for this analysis we choose the tight (T) working point. The JETPROB algorithm [17] determines the probability that the tracks within a jet originate from the primary vertex; we choose for the latter algorithm the loose (L) working point. The efficiency for each b-tagging algorithm is approximately 40%–50%. We require at least one of the first two leading jets in E_T to be tagged by the SECVTX algorithm. Events are further divided among twelve statistically independent subsamples, depending on whether there are no additional b-tagged jets (1T), or an additional jet is tagged by JETPROB but not by SECVTX (TL), or tagged by SECVTX (TT), the number of jets (two-jet or three-jet sample), and the presence or absence of a reconstructed electron or muon. This division increases sensitivity because signal-to-noise ratio and background composition differ across subsamples. The resulting *preselection* sample contains 25 256 events, to which a W' boson with SM-like couplings and 300 GeV/c^2 mass would contribute about 480 events.

The dominant contribution to the preselection sample is due to QCD multijet production. Other processes giving significant contributions are top-antitop quark-pair production ($t\bar{t}$), electroweak single-top-quark production, dibosons (WW, WZ), and production of jets in association with a boson (V + jets, where V stands for a W or a Z boson), including both heavy-flavor jets (from b or c quarks) and jets from light-flavor quarks or gluons that have been erroneously b tagged.

A combination of data and simulations making use of Monte Carlo integration are used to derive the estimates for SM background contributions. The kinematic distributions of events associated with top-quark pair, single-top-quark, V + jets, $W + c$, diboson (VV), and associated Higgs and W or Z boson (VH) production are modeled using simulated samples. The ALPGEN generator [18] is used to model V + jets at leading order in the strong-interaction coupling with up to four partons produced at tree level, based on generator-to-reconstructed-jet matching [19,20]. The POWHEG [21] generator is used to model t- and s-channel single-top-quark production, while PYTHIA [22] is used to model top-quark-pair, VV, and VH production. Each event generator uses the CTEQ5L parton distribution functions [23]. Parton showering is simulated using PYTHIA. Event modeling also includes simulation of the detector response using GEANT [24]. The simulated events are reconstructed and analyzed in the same way as the experimental data. Normalizations of the contributions from t- and s-channel single-top-quark, VV, VH, and $t\bar{t}$ pair production are taken from theoretical cross sections [25–28], while the normalization for $W + c$ production is taken from the measured cross section [29]. For V + jets production, the heavy-flavor contribution is normalized based on the number of b-tagged events observed in an independent data control sample [30]. Contributions of V + jets and VV events containing at least one incorrectly b-tagged light-flavored jet are determined by applying to simulated events a per-event probability, obtained from a generic event sample containing mostly light-flavored jets [31,32]. The efficiency of the trigger-level selection is measured in data and applied to all simulated samples.

Because QCD multijet events with large missing transverse energy are difficult to simulate properly, a suitable model is derived solely from data; we use an independent data sample composed of events with $\Delta\varphi(\vec{\not\!\!E}_T, \vec{E}_T^{j_2}) < 0.4$ and $50 < \not\!\!E_T < 70$ GeV, consisting almost entirely of QCD multijet contributions. First, a b-tagging probability f_i is calculated separately in each b-tagging subsample i

($i = 1\text{T}$, TL , TT) by taking the ratio between tagged and pretagged events as a function of several jet- and event-related variables [33]. Then, QCD multijet kinematic distributions are determined separately for each region i by weighting the untagged data in the preselection sample according to the probability f_i.

The signal is modeled using PYTHIA for W'-boson mass $M_{W'}$ in the range $300 \leq M_{W'} \leq 900\ \text{GeV}/c^2$ in $100\ \text{GeV}/c^2$ increments, where the W' boson is assumed to have purely right-handed decays. As the W'-boson helicity does not affect analysis observables, this model is valid for both a right-handed and a left-handed W' boson under the assumption of no interference with SM W-boson production. Two scenarios are considered, depending on whether the leptonic decay mode $W' \to \ell\nu$ is allowed or forbidden. The latter, for instance, is the case if the hypothetical right-handed neutrino ν_R is more massive than the W' boson. The only effect of the forbidden leptonic decay mode is an increased branching fraction $\mathcal{B}(W' \to tb)$.

As an intermediate background-rejection step, an artificial neural network, NN_{QCD}, is employed to separate the dominant QCD multijet background from signal and other backgrounds. NN_{QCD} is trained using event observables ($\not\!\!E_T$, $\not\!\!p_T$ [34]), angular observables [$\Delta\varphi(\vec{\not\!\!E}_T, \vec{\not\!\!p}_T)$, $\Delta\varphi(\vec{\not\!\!E}_T, \vec{E}_T^{j_i})$, $\Delta\varphi(\vec{\not\!\!p}_T, \vec{E}_T^{j_i})$], and other topological information such as sphericity [35]. As the final-state topologies for a W' boson decaying to a top-bottom quark pair and s-channel single-top-quark production are similar, we employ the same NN_{QCD} function constructed to separate W + jets events from background in the s-channel single-top-quark observation [36]. No information on the W'-boson mass is included in the training sample in order to ensure consistent performance in QCD multijet background separation across the whole W'-boson-mass range under study.

The events must satisfy a minimum NN_{QCD} requirement to maximize sensitivity to single-top-quark s-channel production, which is kinematically very similar to W' production at threshold. The surviving events constitute the *signal* region. To determine the appropriate normalization of QCD events in each analysis subsample, we derive a scale factor in the region composed by the rejected events. Tables I and II show the event yields after the full selection.

We use two additional neural networks, $\text{NN}_{V\text{jets}}$ and $\text{NN}_{t\bar{t}}$, to classify events that satisfy the minimum requirement on the NN_{QCD} output variable. The first neural network, $\text{NN}_{V\text{jets}}$, is trained to separate the W'-boson signal from V + jets and the remaining QCD backgrounds. In the training, a simulated W'-boson signal is used, while the background sample consists of pretag data that satisfy the requirement on NN_{QCD}, reweighted by the tag-rate probability. The second neural network, $\text{NN}_{t\bar{t}}$, is trained to separate the W' boson from $t\bar{t}$ production using simulated samples. Variables that describe the energy and momentum flow in the detector and angular variables are used in the training of the $\text{NN}_{V\text{jets}}$ and $\text{NN}_{t\bar{t}}$ discriminants. The final discriminant, NN_{sig}, is defined as the sum of the square of the $\text{NN}_{V\text{jets}}$ and $\text{NN}_{t\bar{t}}$ output variables, multiplied by appropriate weights optimized to improve the expected sensitivity in each analysis subsample. Figure 1 shows the expected and observed shapes of the NN_{sig} output variable for several subsamples, with the shape corresponding to the $300\ \text{GeV}/c^2$ W' hypothesis overlaid.

A binned likelihood fit is performed to probe a $W' \to tb$ signal in the presence of SM backgrounds. The likelihood is the product of Poisson probabilities over the bins of the NN_{sig} distribution. The mean number of expected events in each bin includes contributions from each background source and from the $W' \to tb$ process assuming a given value of $M_{W'}$. We employ a Bayesian likelihood [37] with a uniform, non-negative prior probability for the W'-boson production cross section times branching fraction, $\sigma(p\bar{p} \to W') \times \mathcal{B}(W' \to tb)$, and truncated Gaussian priors for the uncertainties on the acceptance and shapes of the backgrounds. We combine the twelve signal regions of

TABLE I. Numbers of expected and observed two-jet events with and without identified leptons, combined, in the 1T, TL, and TT subsamples. The uncertainties on the expected numbers of events are due to the theoretical and experimental uncertainties on signal and background modeling. Expected numbers of events for a right-handed W' boson with SM-like couplings and a mass of $300\ \text{GeV}/c^2$ are shown.

Category	1T	TL	TT
s-channel single top	98 ± 10	36.4 ± 3.8	46.1 ± 4.3
t-channel single top	167 ± 24	7.3 ± 1.1	7.9 ± 1.1
$t\bar{t}$	457 ± 32	140.9 ± 11.1	177.4 ± 11.7
VV	259 ± 18	28.5 ± 2.0	27.0 ± 2.0
VH	14 ± 1	5.4 ± 0.5	7.2 ± 0.5
V + jets	3473 ± 901	236.4 ± 61.1	156.7 ± 38.7
QCD	2766 ± 103	220.0 ± 16.8	101.5 ± 12.2
Total background	7235 ± 908	674.3 ± 64.2	524.5 ± 43.0
W' ($300\ \text{GeV}/c^2$)	156 ± 10	59.9 ± 4.6	84.6 ± 7.9
Observed	7128	680	507

TABLE II. Same as in Table I but for three-jet events.

Category	1T	TL	TT
s-channel single top	50 ± 5	13.3 ± 1.5	16.2 ± 1.6
t-channel single top	91 ± 14	5.8 ± 0.9	6.9 ± 1.0
$t\bar{t}$	900 ± 65	148.2 ± 11.6	161.6 ± 10.5
VV	106 ± 8	9.7 ± 0.7	7.8 ± 0.6
VH	6 ± 1	1.7 ± 0.2	2.1 ± 0.2
V + jets	1360 ± 357	80.6 ± 21.2	51.6 ± 13.4
QCD	1261 ± 64	92.8 ± 9.4	31.8 ± 4.6
Total background	3774 ± 369	352 ± 26.3	278 ± 17.5
W' ($300\ \text{GeV}/c^2$)	80 ± 5	23.5 ± 1.9	28.8 ± 3.0
Observed	3613	388	274

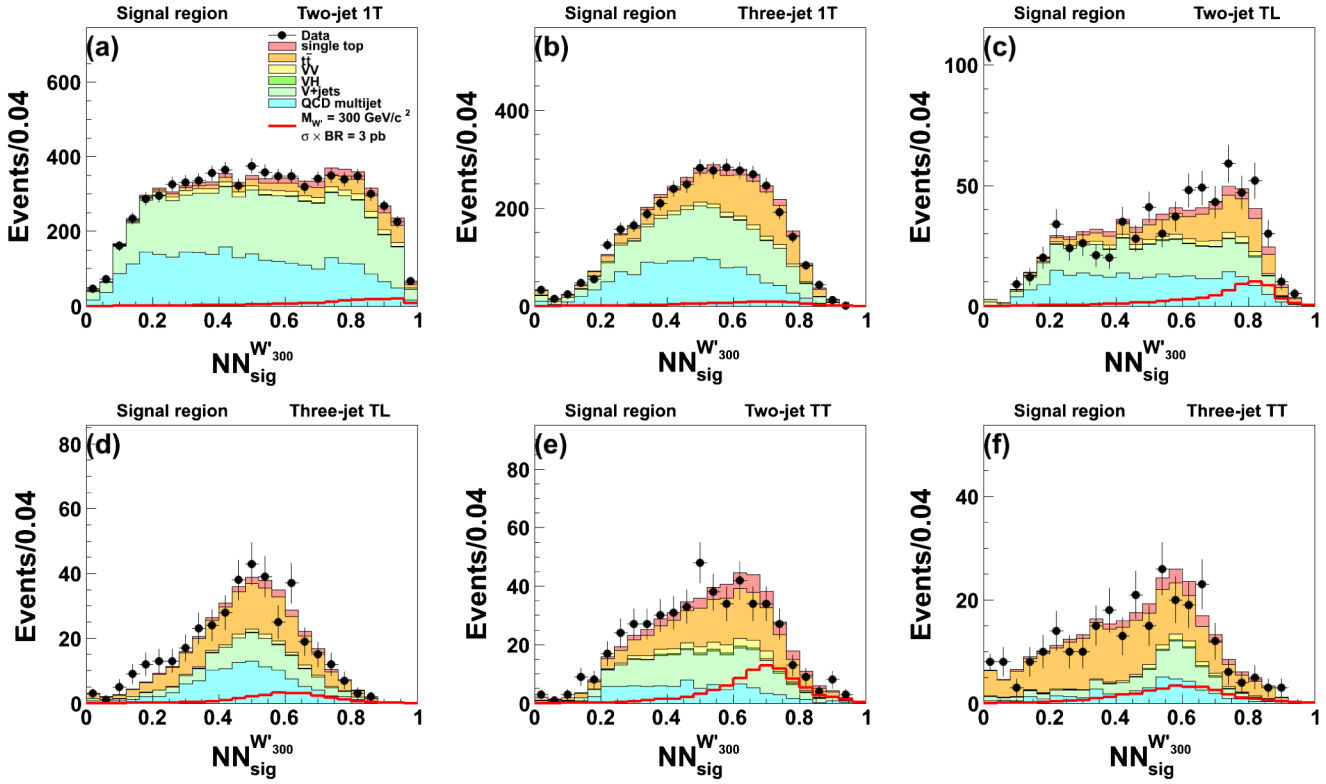

FIG. 1 (color online). Expected and observed final discriminant distributions in the signal region. The distribution for a W' boson with 300 GeV/c^2 mass and SM couplings is overlaid. The signal is normalized to a cross section times branching ratio of 3 pb. Plots show the discriminant in the following subsamples: 1T two-jet (a), 1T three-jet (b), TL two-jet (c), TL three-jet (d), TT two-jet (e), and TT (f) three-jet events.

events characterized by different b-tagging content, jet multiplicity, and presence of well-identified leptons by multiplying the corresponding likelihoods and simultaneously taking into account the correlated uncertainties.

Systematic uncertainties include both uncertainties on template normalization and uncertainties on the shape of the $\mathrm{NN_{sig}}$ distribution. Uncertainties due to the same source are considered 100% correlated. These uncertainties apply to both signal and backgrounds, and include luminosity measurement (6%), b-tagging efficiency (8% to 16%), trigger efficiency (1% to 3%), lepton identification efficiency (2%), parton distribution functions (3%), initial-state and final-state radiation simulation uncertainties (2%) and up to 6% for the jet-energy scale [14]. The uncertainties due to finite simulation sample size, and the uncertainties on the normalization of the production of $t\bar{t}$ (3.5%), t-channel single-top quarks (6.2%), s-channel single-top quarks (5%), dibosons (6%) from the theoretical cross-section calculations [25,26], $W + c$ (23%) from the measured cross section [27,29], and QCD multijet (3% to 100%, calculated from scale factors) are not correlated. The production rates of events with a W or a Z boson plus heavy-flavor jets are associated with a 30% uncertainty. The shapes obtained by varying the b-tagging probability f_i by 1 standard deviation from their central values are applied as uncertainties on the shapes of the QCD background. Changes in the shape of the $\mathrm{NN_{sig}}$ distribution originating from jet-energy-scale uncertainties are also incorporated for processes modeled with simulations. An uncertainty on the b-tagging efficiency due to different performance observed in data and simulations as a function of the jet E_T is applied to signal distributions.

The procedure is performed for all signal mass hypotheses using the methodology described in Ref. [30], obtaining 95% C.L. upper limits on $\sigma(p\bar{p} \to W') \times \mathcal{B}(W' \to tb)$ as a function of $M_{W'}$, assuming no signal present in the data. By comparing the limits on $\sigma(p\bar{p} \to W') \times \mathcal{B}(W' \to tb)$ with the theoretical next-to-leading order calculations for the same quantity for a right-handed W' boson with SM-like couplings [11], we exclude W' bosons for masses less than 860 (880) GeV/c^2 in cases where $W' \to tb$ decay to leptons are allowed (forbidden). The expected and observed upper limits on $\sigma(p\bar{p} \to W') \times \mathcal{B}(W' \to tb)$ divided by theoretical predictions are shown in Fig. 2.

For a simple s-channel-production model with effective coupling $g_{W'}$, and assuming that couplings to light and heavy quarks are identical, the cross section is proportional to $g^2_{W'}$. By relaxing the assumption of universal weak coupling, the limits on the cross section are interpreted as upper limits on $g_{W'}$ as functions of $M_{W'}$. The excluded region of the $g_{W'}$–$M_{W'}$ plane is shown in Fig. 3, with $g_{W'}$ expressed in units of the SM weak couplings, g_W . For a W'

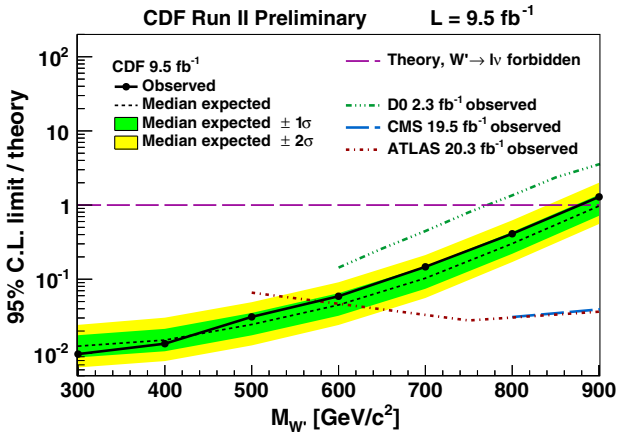

FIG. 2 (color online). Observed (solid line) and expected (dotted line) upper limits on $\sigma(p\bar{p} \to W') \times \mathcal{B}(W' \to tb)$, with $\pm 1\sigma$ and $\pm 2\sigma$ credibility intervals, divided by the theoretical predictions for a right-handed W' boson with SM-like couplings in the scenario where the leptonic decay mode $W' \to \ell\nu$ is forbidden (dashed line). The CDF limits are compared with limits from the latest W' searches from ATLAS, CMS, and D0 [8–10]. The ATLAS (CMS) Collaboration excludes this model for W' masses up to 1.9(2.1) TeV.

boson with a mass of 300 GeV$/c^2$, the effective coupling is constrained at the 95% C.L. to be less than 10% of the W-boson coupling.

In conclusion, we perform a search for a massive resonance decaying to tb with the full CDF II data set, corresponding to an integrated luminosity of 9.5 fb^{-1} . The data are consistent with the background-only hypothesis, and upper limits are set on the production cross section times branching ratio at the 95% Bayesian credibility. For a specific benchmark model (left-right-symmetric SM extension), in cases where the $W' \to tb$ -leptonic-decay mode is allowed (forbidden), we exclude W' bosons with masses lower than 860 (880) GeV$/c^2$. For masses smaller than approximately 600 GeV$/c^2$, this search yields the most constraining limits to date on narrow tb-resonance production.

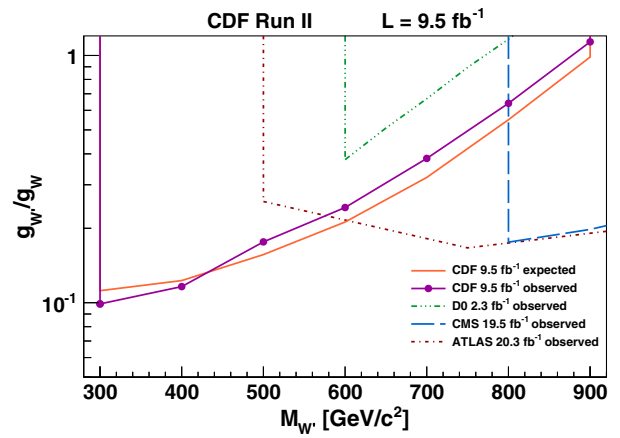

FIG. 3 (color online). Observed and expected 95% C.L. upper limits on the coupling strength of a right-handed W' boson compared to the SM W-boson coupling, $g_{W'}/g_W$, as functions of $M_{W'}$ in cases where the leptonic decay mode $W' \to \ell\nu$ is forbidden. The region above each line is excluded. The CDF limits are compared with limits from the latest W' searches from ATLAS, CMS, and D0 [8–10]. The vertical part in each boundary region of the plot represents the minimum masses for which bounds are quoted.

We thank the Fermilab staff and the technical staffs of the participating institutions for their vital contributions. This work was supported by the U.S. Department of Energy and National Science Foundation; the Italian Istituto Nazionale di Fisica Nucleare; the Ministry of Education, Culture, Sports, Science, and Technology of Japan; the Natural Sciences and Engineering Research Council of Canada; the National Science Council of the Republic of China; the Swiss National Science Foundation; the A. P. Sloan Foundation; the Bundesministerium für Bildung und Forschung, Germany; the Korean World Class University Program, the National Research Foundation of Korea; the Science and Technology Facilities Council and the Royal Society, U.K.; the Russian Foundation for Basic Research; the Ministerio de Ciencia e Innovación, and Programa Consolider-Ingenio, Spain; the Slovak R&D Agency; the Academy of Finland; the Australian Research Council (ARC); and the EU community Marie Curie Fellowship Contract No. 302103.

[*]Deceased.
[a]Visitor from University of British Columbia, Vancouver, BC V6T 1Z1, Canada.
[b]Visitor from Istituto Nazionale di Fisica Nucleare, Sezione di Cagliari, 09042 Monserrato (Cagliari), Italy.
[c]Visitor from University of California Irvine, Irvine, CA 92697, USA.
[d]Visitor from Institute of Physics, Academy of Sciences of the Czech Republic, 182 21, Czech Republic.
[e]Visitor from CERN, CH-1211 Geneva, Switzerland.
[f]Visitor from Cornell University, Ithaca, NY 14853, USA.
[g]Visitor from University of Cyprus, Nicosia CY-1678, Cyprus.
[h]Visitor from Office of Science, U.S. Department of Energy, Washington, DC 20585, USA.
[i]Visitor from University College Dublin, Dublin 4, Ireland.
[j]Visitor from ETH, 8092 Zürich, Switzerland.
[k]Visitor from University of Fukui, Fukui City, Fukui Prefecture, Japan 910-0017.
[l]Visitor from Universidad Iberoamericana, Lomas de Santa Fe, México, C.P. 01219, Distrito Federal.
[m]Visitor from University of Iowa, Iowa City, IA 52242, USA.
[n]Visitor from Kinki University, Higashi-Osaka City, Japan 577-8502.
[o]Visitor from Kansas State University, Manhattan, KS 66506, USA.

[p]Visitor from Brookhaven National Laboratory, Upton, NY 11973, USA.
[q]Visitor from Istituto Nazionale di Fisica Nucleare, Sezione di Lecce, Via Arnesano, I-73100 Lecce, Italy.
[r]Visitor from Queen Mary, University of London, London, E1 4NS, United Kingdom.
[s]Visitor from University of Melbourne, Victoria 3010, Australia,
[t]Visitor from Muons, Inc., Batavia, IL 60510, USA.
[u]Visitor from Nagasaki Institute of Applied Science, Nagasaki 851-0193, Japan,
[v]Visitor from National Research Nuclear University, Moscow 115409, Russia.
[w]Visitor from Northwestern University, Evanston, IL 60208, USA.
[x]Visitor from University of Notre Dame, Notre Dame, IN 46556, USA.
[y]Visitor from Universidad de Oviedo, E-33007 Oviedo, Spain.
[z]Visitor from CNRS-IN2P3, Paris, F-75205 France.
[aa]Visitor from Universidad Tecnica Federico Santa Maria, 110v Valparaiso, Chile.
[bb]Visitor from The University of Jordan, Amman 11942, Jordan.
[cc]Visitor from Universite catholique de Louvain, 1348 Louvain-La-Neuve, Belgium.
[dd]Visitor from University of Zürich, 8006 Zürich, Switzerland.
[ee]Visitor from Massachusetts General Hospital, Boston, MA 02114, USA.
[ff]Visitor from Harvard Medical School, Boston, MA 02114, USA.
[gg]Visitor from Hampton University, Hampton, VA 23668, USA.
[hh]Visitor from Los Alamos National Laboratory, Los Alamos, NM 87544, USA.
[ii]Visitor from Università degli Studi di Napoli Federico I, I-80138 Napoli, Italy.

[1] J. C. Pati and A. Salam, Phys. Rev. D **10**, 275 (1974).
[2] Y. Mimura and S. Nandi, Phys. Lett. B **538**, 406 (2002).
[3] G. Burdman, B. A. Dobrescu, and E. Ponton, Phys. Rev. D **74**, 075008 (2006).
[4] H. Georgi, E. E. Jenkins, and E. H. Simmons, Nucl. Phys. **B331**, 541 (1990).
[5] E. Malkawi, T. M. Tait, and C. Yuan, Phys. Lett. B **385**, 304 (1996).
[6] M. Perelstein, Prog. Part. Nucl. Phys. **58**, 247 (2007).
[7] T. Aaltonen *et al.* (CDF Collaboration), Phys. Rev. Lett. **103**, 041801 (2009).
[8] V. M. Abazov *et al.* (D0 Collaboration), Phys. Lett. B **699**, 145 (2011).
[9] G. Aad *et al.* (ATLAS Collaboration), Phys. Lett. B **743**, 235 (2015).
[10] S. Chatrchyan *et al.* (CMS Collaboration), J. High Energy Phys. 05 (2014) 108.
[11] Z. Sullivan, Phys. Rev. D **66**, 075011 (2002).
[12] D. Acosta *et al.* (CDF Collaboration), Phys. Rev. D **71**, 032001 (2005).
[13] CDF II uses a cylindrical coordinate system with azimuthal angle f, polar angle θ measured with respect to the positive z direction along the proton beam, and distance r measured from the beam line. The pseudorapidity, transverse energy, and transverse momentum are defined as $\eta = -\ln[\tan(\theta/2)]$, $E_T = E\sin\theta$, and $p_T = p\sin\theta$, respectively, where E and p are the energy and momentum of an outgoing particle. The missing transverse energy $\vec{E}_T$ is defined by $\vec{E}_T = -\sum_i E_T^i \hat{n}_i$, where $\hat{n}_i$ is a unit vector perpendicular to the beam axis that points to the ith calorimeter tower ($\not{E}_T = |\vec{E}_T|$). The missing transverse momentum $\not{p}_T$ is analogously defined starting from the momenta of reconstructed charged particles as measured by the spectrometer.
[14] A. Bhatti *et al.*, Nucl. Instrum. Methods Phys. Res., Sect. A **566**, 375 (2006).
[15] C. Adloff *et al.* (H1 Collaboration), Z. Phys. C **74**, 221 (1997).
[16] D. Acosta *et al.* (CDF Collaboration), Phys. Rev. D **71**, 052002 (2005).
[17] A. Abulencia *et al.* (CDF Collaboration), Phys. Rev. D **74**, 072006 (2006).
[18] M. L. Mangano, M. Moretti, F. Piccinini, R. Pittau, and A. D. Polosa, J. High Energy Phys. 07 (2003) 001.
[19] M. L. Mangano, M. Moretti, F. Piccinini, and M. Treccani, J. High Energy Phys. 01 (2007) 013.
[20] J. Alwall *et al.*, Eur. Phys. J. C **53**, 473 (2008).
[21] S. Alioli, P. Nason, C. Oleari, and E. Re, J. High Energy Phys. 06 (2010) 043.
[22] T. Sjöstrand, S. Mrenna, and P. Z. Skands, J. High Energy Phys. 05 (2006) 026.
[23] H. Lai *et al.* (CTEQ Collaboration), Eur. Phys. J. C **12**, 375 (2000).
[24] R. Brun, F. Carminati, and S. Giani, Report No. CERN-W-5013, 1994.
[25] N. Kidonakis, Phys. Rev. D **81**, 054028 (2010).
[26] J. M. Campbell and R. K. Ellis, Phys. Rev. D **60**, 113006 (1999).
[27] J. Baglio and A. Djouadi, J. High Energy Phys. 10 (2010) 064.
[28] P. Bärnreuther, M. Czakon, and A. Mitov, Phys. Rev. Lett. **109**, 132001 (2012).
[29] T. Aaltonen *et al.* (CDF Collaboration), Phys. Rev. Lett. **110**, 071801 (2013).
[30] T. Aaltonen *et al.* (CDF Collaboration), Phys. Rev. D **82**, 112005 (2010).
[31] D. Acosta *et al.* (CDF Collaboration), Phys. Rev. D **71**, 052003 (2005).
[32] A. Abulencia *et al.* (CDF Collaboration), Phys. Rev. D **74**, 072006 (2006).
[33] T. Aaltonen *et al.* (CDF Collaboration), Phys. Rev. Lett. **109**, 111805 (2012).
[34] M. Bentivegna, Q. Liu, F. Margaroli, and K. Potamianos, arXiv:1205.4470.
[35] The event sphericity is defined by $S = \frac{3}{2}(\lambda_2 + \lambda_3)$, where the sphericity tensor is $S^{\alpha\beta} = (\sum_i p_i^\alpha p_i^\beta)/(\sum_i p_i^2)$ and $\lambda_1 > \lambda_2 > \lambda_3$ are its three eigenvalues and satisfy $\lambda_1 + \lambda_2 + \lambda_3 = 1$. The index i refers to each jet in the event.
[36] T. A. Aaltonen *et al.* (CDF Collaboration and D0 Collaboration), Phys. Rev. Lett. **112**, 231803 (2014).
[37] K. Olive *et al.* (Particle Data Group), Chin. Phys. C **38**, 090001 (2014).